The EMBO Journal Vol.18 No.12 pp.3305–3316, 1999

Drainin required for membrane fusion of the contractile vacuole in *Dictyostelium* is the prototype of a protein family also represented in man

Michael Becker, Monika Matzner and Günther Gerisch[1]

Max-Planck-Institut für Biochemie, D-82152 Martinsried, Germany

[1]Corresponding author
e-mail: gerisch@biochem.mpg.de

The contractile vacuole expels water by forming a channel with the plasma membrane and thus enables cells to survive in a hypo-osmotic environment. Here we characterize drainin, a *Dictyostelium* protein involved in this process, as the first member of a protein family represented in fission yeast, *Caenorhabditis elegans* and man. Gene replacement in *Dictyostelium* shows that drainin acts at a checkpoint of channel formation between the contractile vacuole and the plasma membrane. A green fluorescent protein fusion of drainin localizes specifically to the contractile vacuole and rescues its periodic discharge in drainin-null cells. Drainin is a peripheral membrane protein, requiring a short hydrophobic stretch in its C-terminal region for localization and function. We suggest that drainin acts in a signaling cascade that couples a volume-sensing device in the vacuolar membrane to the membrane fusion machinery.

Keywords: functional genomics/green fluorescent protein/membrane fusion/osmoregulation/restriction enzyme-mediated insertion

Introduction

Membrane fusion is essential for intracellular transport processes and cell interactions such as endoplasmic reticulum (ER) to Golgi transport, release of neurotransmitters and hormones, the acrosome reaction in fertilization, and virus entry (Skehel and Wiley, 1988; Rothman, 1994; Benett, 1995; Allen and Green, 1997; Hughson, 1997). A ubiquitous fusion machinery consists of three highly conserved protein families, referred to as SNAREs (SNAP receptors), SNAPs (soluble NSF attachment proteins) and NSF (*N*-ethylmaleimide-sensitive factor) (Hanson *et al*., 1997; Geppert and Südhof, 1998; Sato and Wickner, 1998; Weber *et al*., 1998). In addition to these principal proteins, various classes of other proteins assist or regulate membrane fusion (Xu *et al*., 1998). These proteins include cystein string proteins (Umbach *et al*., 1995), members of the Rab family of small GTPases (Rybin *et al*., 1996), annexins (Emans *et al*., 1993; Caohuy *et al*., 1996), Ca^{2+} sensors (Schiavo *et al*., 1995) and proteins regulating actin polymerization (Muallem *et al*., 1995; Zhang *et al*., 1996).

A special system for studying membrane fusion is the contractile vacuole in protozoans that live within a hypo-osmotic environment such as fresh water or soil. To fulfill its function as an osmoregulatory organelle, the contractile vacuole fuses periodically with the plasma membrane to expel water from the cell body. The membranes of the contractile vacuole system are decorated with a vacuolar type of proton pump, which provides the driving force for filling the vacuole by transporting protons from the cytoplasm into the lumen (Heuser *et al*., 1993; Nolta and Steck, 1994; Liu and Clarke, 1996). Bicarbonate ions are considered to combine with the translocated protons to generate the water, which is pumped out during vacuole discharge (Giglione and Gross, 1995; Clarke and Heuser, 1997).

In *Dictyostelium*, the contractile vacuole system consists of an intracellular network of cisternae and interconnecting ducts (Heuser *et al*., 1993). The largest cisternae are the contractile vacuoles, also called bladders (Nolta and Steck, 1994). Cisternae and connecting ducts are interconvertible (Gingell *et al*., 1982). Ducts associated with a contractile vacuole disappear when the vacuole expands, apparently by incorporation of the duct membranes into the vacuolar membrane (Heuser *et al*., 1993).

The contractile vacuole system provides an excellent model to study the regulated and reversible formation of membrane channels. Despite the abundant knowledge accumulated on the organization of this system (Clarke and Heuser, 1997), there is a lack of mutations that selectively block contractile vacuole activity. Restriction enzyme-mediated insertion (REMI; Kuspa and Loomis, 1992) was used for shotgun mutagenesis to identify proteins that play a central role in the dilatation/contraction cycle of the contractile vacuole. As a first step in defining the molecular mechanism of the regulated channel formation between the vacuole and the plasma membrane, we characterize here a mutation that impairs vacuole discharge. The gene disrupted by REMI encodes a protein that specifically associates with the contractile vacuole. By tagging the protein with green fluorescent protein (GFP), we show that this association is essential for the periodic fusion of the vacuole with the plasma membrane. We name the protein drainin because of its requirement for water expulsion from the vacuole. Drainin turned out to be the first functionally characterized member of a family also represented in *Schizosaccharomyces pombe*, *Caenorhabditis elegans* and man.

Results

Drainin is responsible for the discharge of contractile vacuoles

In a multipurpose screen for mutants deficient in activities of the cell cortex during growth or development, we subjected the *D.discoideum* strain HG592 (Gerisch *et al*., 1985) to REMI mutagenesis and checked the clones by microscopic inspection. One of the checked mutants was

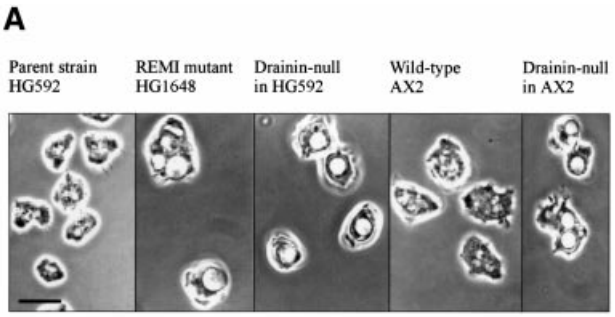

B

```
  1  MICFDNSTAHTDSNNNNNQCDLPENYKELVTTGKVEKLIL  40
 41  SPSSSLDRPKTLPPKSQEEVLKHQREYEEIQRKAKKTLER  80
 81  EAKEKEKLDAIRKEKERSLIDARKVWEEDIIPVWEKNSKK 120
121  RDIKKIKDLSWRGLPPAVRGKIWRLCIGNDLRVTDELFNI 160
161  FLGHANNAYNKTTSPPLKSSLSSSSKSPNINIDLRQANNS 200
201  IHHSRSPMNTSTDGEDDVLDLETTNMALILQDIQDTFPSL 240
241  MIFQKGGPLHSDLIDVLGAYICYRPDIGYVPGMTFLAAMF 280
281  LLNMEKCDAFLSLSNHINSVCFLPFFRQDQSGIPKYLAAM 320
321  DSTVEALTPPLHKHFKEIGISAKNYLVDWITTLFSKALPL 360
361  DVATTIWDLVFIEGEIFIYRTALSILRYFISDLIQATYDE 400
401  CIDLFNKLPQRKISEDKLFEEIQSIVLDQRKFDKLLEK   438
```

Fig. 1. Expanded vacuoles in drainin gene disruption and replacement mutants (A) and amino acid sequence of drainin (B). (**A**) The *D.discoideum* strain HG592 mutagenized by REMI yielded the disruption mutant HG1648. The dependence of the phenotype on inactivation of the drainin gene was established by targeted gene replacement in HG592 and the wild-type AX2 strain. Bar = 10 μm. (**B**) In the drainin sequence, five heptad repeats are boxed and a hydrophobic stretch is underlined. The open arrowhead points to the site of gene disruption in HG1648; the closed arrowheads indicate the sequence eliminated in gene replacement mutants. The genomic drainin sequence received DDBJ/EMBL/GenBank accession No. U81500.

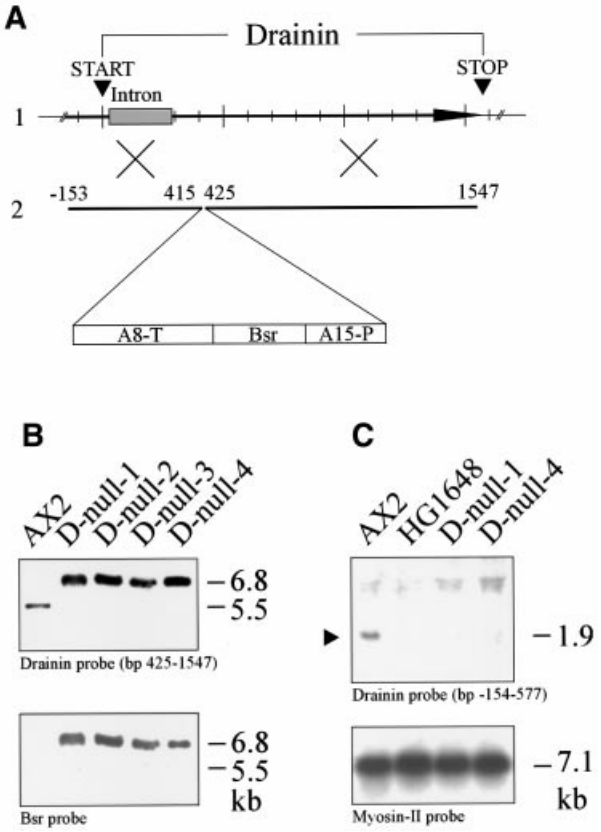

Fig. 2. Construction of the drainin gene replacement vector (A), and analysis of knock-out mutants by Southern (B) and Northern blotting (C). (**A**) In the genomic sequence of drainin (1), a resistance cassette was inserted comprising the actin 15 promoter (A15-P), the blasticidin deaminase-coding region (Bsr) and the actin 8 terminator (A8-T). (**B**) Southern blot showing single integration of the Bsr cassette into the drainin gene. Genomic DNA was digested with *Cla*I. In the upper panel, the blot was hybridized with a 3′ probe of the drainin gene, showing an up shift of the fragment by 1.3 kb in the drainin-null mutants, corresponding to the size of the Bsr cassette. In the lower panel, the blot was hybridized with a Bsr probe. Only a single band was labeled in each of the mutants, which coincided with the shifted drainin band. (**C**) Northern blot showing the drainin transcript in the wild-type (closed arrowhead) and no detectable transcript in representative mutants. The upper blot was exposed for 2 weeks in order to recognize the transcript in wild-type cells, indicating low abundance of the drainin message. Lack of polyadenylation signals is most probably the reason why no truncated transcript was found in the mutants. The lower blot shows, as a reference for equal loading, the heavy chain transcript of myosin II. Numbers are sizes interpolated from marker positions. D-null-1 and D-null-2 are two independent gene replacement mutants in the AX2 background, D-null-3 and D-null-4 are two independent mutants in the HG592 background.

characterized by typically one or two extremely dilated vacuoles (Figure 1A). The protein encoded by the disrupted gene comprises 438 amino acid residues with a calculated molecular mass of 50 kDa (Figure 1B). The N-terminal half of the protein contains five heptad repeats with a high capacity for forming a coiled-coil structure. The C-terminal portion includes a cluster of eight hydrophobic amino acids. In the Discussion, we will compare the sequence of this *Dictyostelium* protein, that we named drainin, with sequences encoded in other eukaryotes.

To verify that the disordered vacuole function is due to disruption of the cloned gene, we have generated mutants by targeted gene replacement in the original parent HG592 and in the AX2 strain of *D.discoideum*, designated here as wild type. In both the HG592 and wild-type strains, interruption of the drainin gene led to the same phenotype as the initial REMI mutation (Figure 1A). Southern blots established that in eight independent mutants analyzed, the construct used for gene replacement integrated into the drainin gene (Figure 2A and B). Northern blots revealed the presence of a 1.9 kb transcript in wild type, and no detectable message in the replacement mutants tested (Figure 2C). All the following experiments were performed with mutant D-null-1.

To identify the dilated vacuoles in drainin-null mutants as inactive contractile vacuoles, cells were labeled with antibody against calmodulin, which is strongly enriched at the contractile vacuole (Zhu and Clarke, 1992). The antibody decorated the dilated vacuoles in the mutant (Figure 3A) as heavily as it decorated the contractile vacuoles in wild type. The mutant vacuoles were also labeled with antibody against the 70 kDa subunit of vacuolar H^+-ATPase (Figure 3B). This proton pump is abundant in membranes of the contractile vacuole complex but is also present at the membranes of acidic endosomes (Heuser *et al*., 1993).

No gross alteration in ultrastructure was recognized in drainin-null cells, except that the vacuole was spread extensively beneath the cell surface, indicating a tight connection between the plasma and vacuolar membranes (Figure 3C and D). Electron micrographs revealed a space

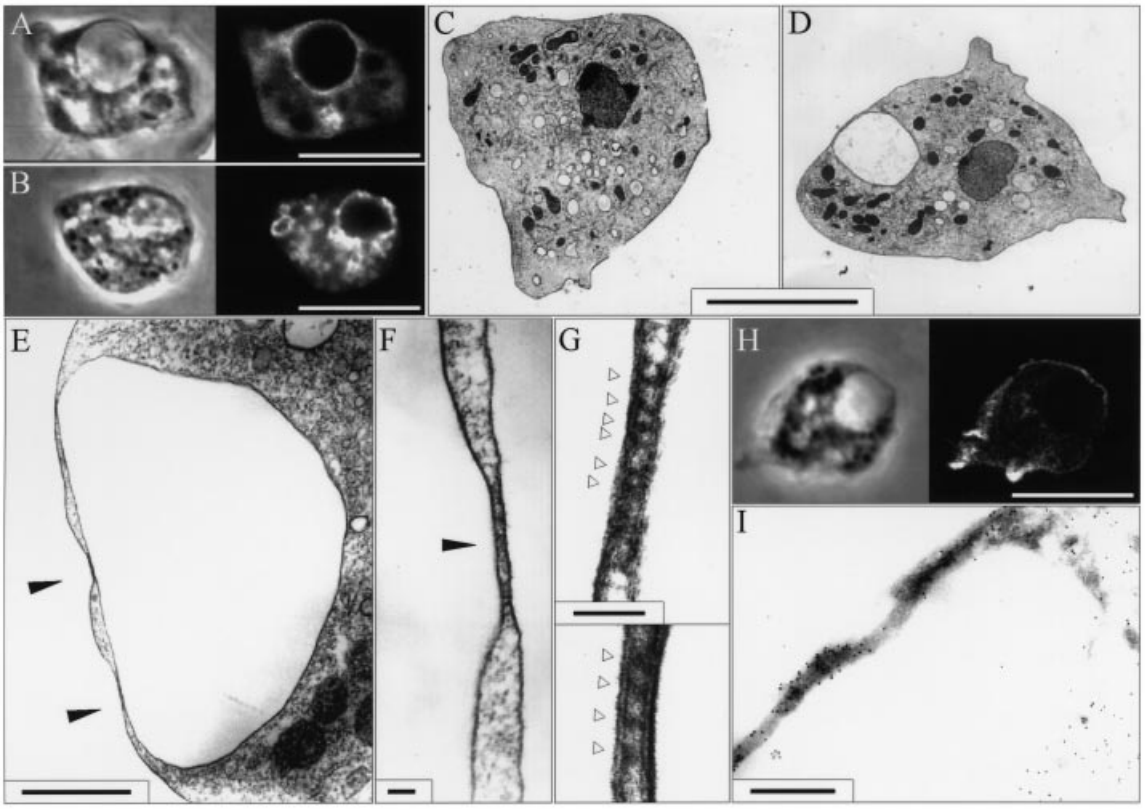

Fig. 3. Blocked discharge of contractile vacuoles in drainin-null cells. (**A**) The expanded vacuoles in the mutant cells were identified as contractile vacuoles by labeling with calmodulin antibody. (**B**) Vacuolar H^+-ATPase, common to the contractile vacuole and endosome systems, decorates the giant vacuole in drainin-null cells in addition to other vesicles. (**C**) A wild-type control cell and (**D**) a drainin-null cell showing no gross alteration in cell ultrastructure associated with the impairment of contractile vacuole activity. (**E**–**G**) The contractile vacuole spread beneath the surface of drainin-null cells is separated from the plasma membrane by a cytoplasmic space of variable thickness. Regions of closest approximation of the membranes are indicated by closed arrowheads, and palisade-like arrays of proteins between the membranes by open arrowheads in (G).
(**H** and **I**) The presence of actin in the space between the vacuolar and plasma membrane is demonstrated with TRITC–phalloidin (H) or actin immunogold labeling (I). In (A), (B) and (H), phase-contrast images are compared with confocal fluorescence images of the same cells. In (C–G), ultrathin sections of Epon-embedded cells are shown, and in (I) a cryosection indirectly gold-labeled using anti-actin antibody. Bars = 10 μm (in A, B and H), 5 μm (in C and D), 1 μm (in E), 50 nm (in F and G) and 500 nm (in I).

between the membranes that varied in thickness between 20 and 50 nm (Figure 3E and F). At the areas of closest proximity between these membranes, electron-dense structures were recognizable that connected the cytoplasmic phases of the two membranes in a palisade-like array (Figure 3G). Labeling with phalloidin indicated the presence of actin filaments in the intermembrane space (Figure 3H). Immunogold labeling of cryosections confirmed the presence of an actin layer between the vacuolar and plasma membranes (Figure 3I).

Drainin-null cells are sensitive to hypo-osmotic shock

To examine whether impairment of the contractile vacuole makes drainin-null cells sensitive to up or down shifts of osmolality, wild-type and mutant cells were challenged by replacing nutrient medium, that had an osmolality of ~130 mosm, either by distilled water, 17 mM phosphate buffer (30 mosm) pH 6.0, or by 400 mM sorbitol in the same buffer. As an iso-osmotic control, cells were transferred into a solution of 130 mM sucrose in the 17 mM phosphate buffer.

Microscopic observation revealed that upon transfer into a hypo-osmotic environment, a portion of the mutant cells visibly lysed. To quantify the survival rates, cells incubated for 2 h under the different osmotic conditions were transferred onto agar plates with bacteria and the emanating colonies were counted. On transfer into water, the survival rate was diminished by 63% in comparison with iso-osmotic sucrose. In the hypo-osmotic phosphate buffer, survival was reduced by 22%, whereas the hyper-osmotic sorbitol buffer preserved viability as well as the iso-osmotic sucrose (Figure 4A). These results indicate that drainin-null cells are sensitive specifically to down shifts of osmolality.

The drainin-null phenotype points to a sensor for vacuole size in the wild-type

In order to specify the defect in the vacuole activity of drainin-null cells, wild-type and mutant cells were monitored by video imaging, and quantitative data were extracted from the time series. In wild-type cells, the vacuoles reached essentially the same final sizes in nutrient medium and phosphate buffer, but the pumping frequencies were different (Table I). After transfer of the cells from nutrient medium into phosphate buffer, the intervals between two discharges were shortened from an average of 3 min to 22 s. These results indicate that discharge is initiated when a defined volume of the vacuole is reached. This volume is not determined by a limited mechanical

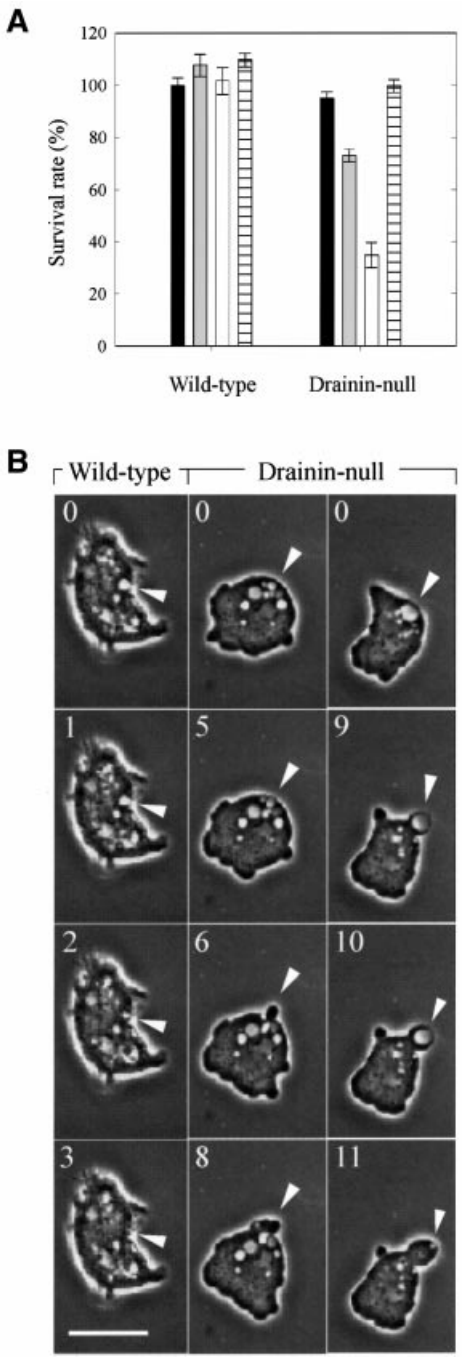

Fig. 4. Sensitivity of drainin-null cells to hypo-osmotic shock. (**A**) Survival rates of wild-type and drainin-null cells transferred from nutrient medium into buffers of different osmolality. Cells were incubated in 130 mM sucrose in 17 mM K/Na phosphate buffer, pH 6.0 (black colums), in the same buffer without sucrose (gray), in water (white) or in 400 mM sorbitol in the phosphate buffer (hatched). After 2 h of incubation under these conditions, cells were plated onto nutrient agar plates with bacteria. Colony-forming units are pooled from five independent experiments, and bars indicate SEM. Data are plotted relative to the wild-type values of cells incubated in 130 mM sucrose; the mean of these values was set at 100%. (**B**) Discharge of contractile vacuoles in a wild-type cell and two drainin-null cells transferred to 17 mM K/Na phosphate buffer, pH 6.0. Numbers refer to seconds after the first image. Arrowheads point to sites of vacuole discharge. Bar = 10 μm.

capacity of the vacuoles to expand, since in drainin-null cells vacuoles became >10-fold larger than in wild-type cells. We propose, therefore, a volume sensor at the vacuolar membrane that generates a signal for fusion with the plasma membrane, and that drainin controls one step in this process.

In drainin-null cells cultivated in nutrient medium, no discharge was observed within 1–5 h periods of recording. The only exceptions were cells which entered mitosis during the period of observation. In these cells, we saw that large vacuoles became fragmented and finally emptied at a late stage of cell division. In interphase cells, discharges of vacuoles were only observed upon a down shift in osmolality. The intervals of these discharges proved to be extremely variable, ranging from 10 s to 30 min. This variability was due to the atypical way in which the vacuoles expelled their contents. Whereas wild-type cells needed 3–5 s until discharge was completed (Figure 4B, left panel), the vacuoles in drainin-null cells collapsed within <1 s, indicating that the fluid was not pressed through a channel but released by rupture of the membranes. This rupture is illustrated by the two mutant cells shown in Figure 4B, middle and right panels. In one of them, a bleb was formed at the site of the vacuole, turning the inner part of the vacuolar membrane to the outside. In the other cell, the vacuole was evaginated before it emptied. In both cases, the formation of a channel was replaced by mechanical perforation of the thin lamella separating the vacuole from the plasma membrane.

In order for drainin-null cells to survive under hypo-osmotic conditions, rapid resealing of the ruptured membranes is indispensable. The ability of mutant cells to seal a gap between the vacuole and plasma membranes was demonstrated by perforating the lamella on top of a vacuole with a fine glass needle. The contents of the punctured vacuoles were released, but the cells survived. This is in contrast to cells lysing immediately as a result of piercing through other parts of the plasma membrane (data not shown).

GFP–drainin rescues osmoregulation by associating with the contractile vacuoles

The site of drainin action was identified by complementing drainin-null cells with full-length drainin tagged at its N-terminus with GFP. In the complemented cells, the contractile vacuoles were active and reached normal sizes before discharge. The fusion protein decorated one, or sometimes a few, vacuoles within each cell (Figure 5A). The plasma membrane was not labeled detectably, but there was a background of fluorescence in the cytoplasm.

The association of GFP–drainin with the vacuolar membrane strictly depended on the presence of the hydrophobic stretch of amino acid residues 275–282 (Figure 1B). When this stretch was deleted, only diffuse fluorescence in the cytoplasm was observed (Figure 5A). The vacuoles remained large and did not fuse with the plasma membrane. The same was true in drainin-null cells producing free GFP only (Figure 5A). Western blots labeled with anti-GFP antibody confirmed that the GFP fusions had the size predicted from the calculated molecular mass, i.e. 78 kDa for the full-length fusion protein or 77 kDa for the fusion protein lacking the hydrophobic stretch

Table I. Volume and period of discharge of contractile vacuoles in wild-type and drainin-null mutants

Strain	Environment	Volume (μm^3) of contractile vacuoles[a]	Discharge period (s)[b]
Wild-type AX2	Nutrient medium	1.1 ± 0.1 (0.4)	189.4 ± 24.2 (102.6)
Wild-type AX2	phosphate buffer	1.3 ± 0.1 (0.6)	22.9 ± 4.2 (16.1)
Drainin-null	nutrient medium	14.8 ± 2.3 (14.7)	no discharge observed[c]
Drainin-null	phosphate buffer	20.4 ± 5.0 (27.4)	164.9 ± 54.3 (311.8)

[a]Volumes were calculated using the measured diameter of round vacuoles or the average of large and small diameters of crescent-shaped vacuoles. Mean ± SEM (SD), $n = 100$.
[b]Determined by videomicroscopy. Mean ± SEM (SD), $n = 100$.
[c]With the exception of late phases in mitotic cell division.

(Figure 5B). No degradation products containing the N-terminal GFP moiety were detected.

To establish that GFP–drainin fully rescues vacuole function in drainin-null cells and that association with the vacuolar membranes is necessary for drainin activity, the osmo-sensitivity of the transfected cells was assayed. Only the full-length GFP–drainin restored resistance to hypo-osmotic shock (Figure 5C).

Fractionation of cell lysates showed that drainin exists in a membrane-bound and a cytosolic state. In the presence of 1 M NaCl or 0.1 M sodium carbonate, GFP–drainin was solubilized quantitatively (Figure 5D), indicating that drainin is a peripheral membrane protein. Calnexin, an integral membrane protein of the ER, was labeled in parallel and remained strictly associated with the membrane fraction under both conditions. By treatment with 1% Triton X-100, calnexin was completely and drainin partially solubilized.

No impairment of endocytic trafficking is detected in drainin-null cells

To examine whether membrane fusion in the endocytic pathway is affected by the lack of drainin, cells were labeled with tetramethylrhodamine isothiocyanate (TRITC)–dextran, which is taken up into endosomes by macropinocytosis (Hacker *et al*., 1997). The loaded endosomes were separated sharply from the expanded vacuoles in the mutant cells (Figure 6A). This means that endocytic vesicles were not enlarged in drainin-null cells, and that these vesicles did not fuse with the expanded contractile vacuole.

Neutral red accumulates in the acidic lysosomes of living cells. Because proton pumps are supplied to endosomes by their fusion with vesicles that have stored H^+-ATPase in their membranes (Cardelli *et al*., 1989; Nolta *et al*., 1994), neutral red labeling proves that this fusion has occurred. In drainin-null cells, neutral red-labeled vesicles were found as in wild-type cells, which indicates that drainin is not required for membrane fusion at the early phase of endocytic trafficking (Figure 6B).

Vacuolins A and B are markers for the post-lysosomal stage of endosomes (Jenne *et al*., 1998). The vesicles decorated with anti-vacuolin antibodies appeared to be of normal size, clearly distinguishable from the huge vacuoles of the drainin-null cells (Figure 6C). This result differentiates drainin-null cells from cells lacking vacuolin B, in which acidic lysosomes are enlarged (Jenne *et al*., 1998).

As a quantitative assay for endocytic trafficking of wild-type and drainin-null mutants, cells were loaded with TRITC–dextran for 3 h, a period more than sufficient to reach an equilibrium between uptake and release of this endosomal marker (Cardelli *et al*., 1989; Jenne *et al*., 1998). After transfer of the cells into fresh medium, release of the marker by exocytosis was determined by fluorimetry. No difference in the rate of exocytosis between wild-type and drainin-null cells was found (Figure 6D). This result distinguishes drainin-null cells from cells lacking vacuolin B, in which exocytosis is delayed (Jenne *et al*., 1998).

In accord with the highly specific requirement for drainin on the contractile vacuole and its action in protecting cells against hypo-osmotic shock, the growth rate of drainin-null mutants was similar to the growth rate of wild-type cells. In nutrient medium, the generation time was 8.2 h for wild-type and 8.6 h for mutant cells. Neither were generation times significantly altered by the absence of drainin during growth on bacteria suspended in 17 mM phosphate buffer; generation times were 2.6 h for wild-type and 2.8 h for mutant cells. Drainin-null mutants were also capable of undergoing multicellular development up to the final stage of fruiting body formation.

Drainin distinguishes the contractile vacuole from the endocytic pathway

To underline the distinction of contractile vacuoles decorated with GFP–drainin from vesicles of the endocytic pathway, vacuoles were monitored during all phases of their contraction/dilatation cycle. After discharge, a patch of GFP–drainin remained concentrated at the site of the emptied vacuole. This was particularly clear in the images of vacuoles that emptied within the confocal plane (Figure 7A). No spreading of GFP–drainin along the plasma membrane was observed.

Since GFP–drainin persistently marked the contractile vacuoles, it was possible to show that these vacuoles remained separate through all phases of their activities from the endosomal compartment. The endosomes were fully labeled in cells complemented with GFP–drainin by pre-incubation with TRITC–dextran for 3 h. In Figure 7B, the loaded endosomes are clearly distinguishable from the vacuoles decorated with GFP–drainin. In no phase of the contraction/dilatation cycle could we detect TRITC–dextran within the vacuoles decorated with GFP–drainin.

Discussion

The drainin family of eukaryotic proteins

Here we report on the discovery of drainin, a *Dictyostelium* protein involved in the regulation of channel formation

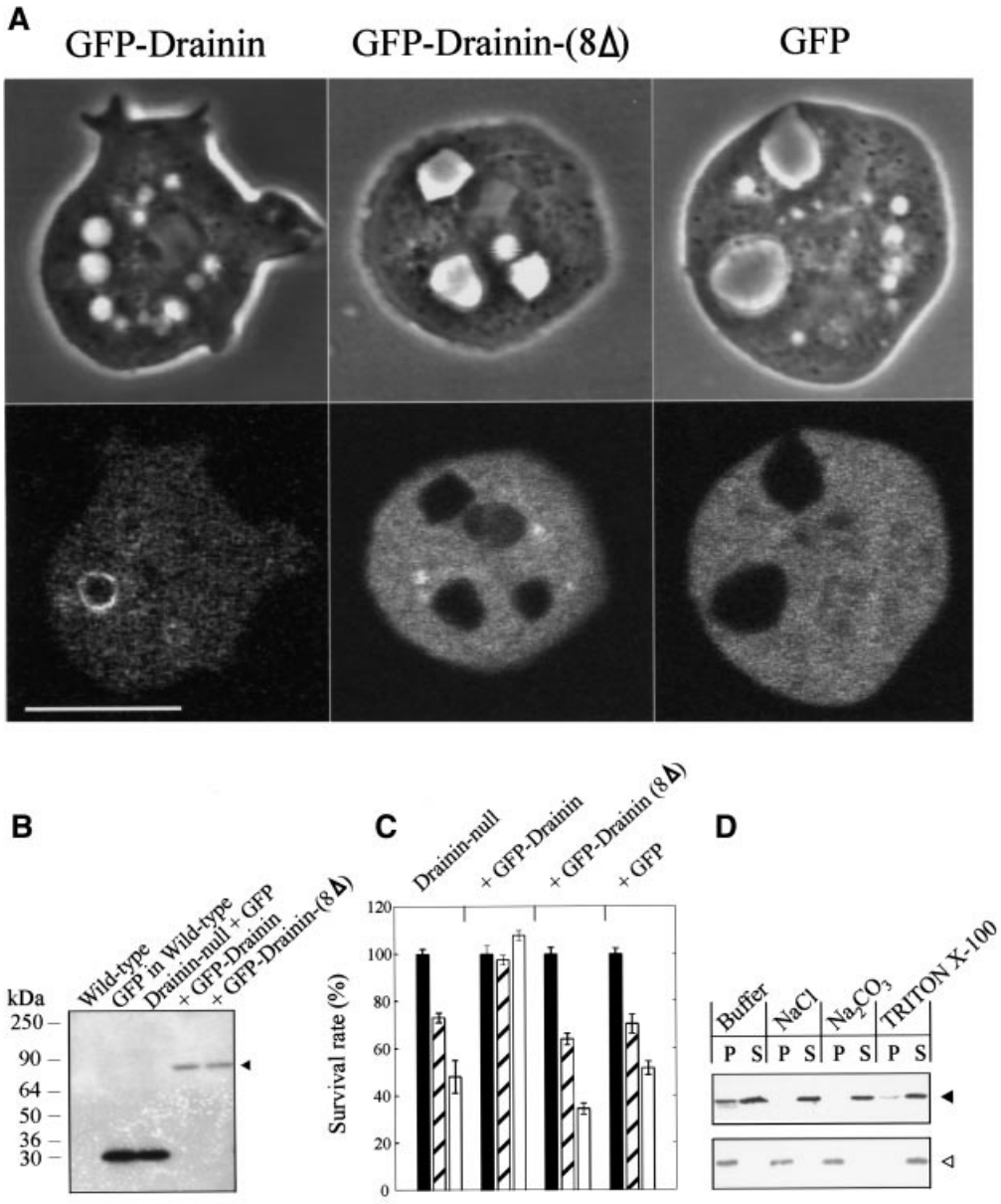

Fig. 5. Rescue of drainin-null cells by membrane-associated GFP–drainin. (**A**) Drainin-null cells complemented with GFP fusions of full-length drainin (left), drainin lacking the stretch of eight hydrophobic amino acids in the C-terminal region (middle) or free GFP (right). Only full-length drainin decorates the vacuolar membrane. Bar = 10 μm. (**B**) Western blot of total cell lysates labeled with anti-GFP antibody. The positions of GFP–drainin fusion proteins are indicated by the arrowhead. (**C**) Survival rate of cells transferred from nutrient medium to 130 mM sucrose in phosphate buffer (filled columns), to 17 mM buffer alone (hatched columns) or to water (open columns). Conditions were the same as in Figure 4. Data ± SEM are from five experiments. Survival rates in sucrose are set at 100% in the drainin-null mutant and in each of the complemented strains shown in (A). (**D**) Fractionation of full-length GFP–drainin (closed arrowhead) and calnexin (open arrowhead), a reference integral membrane protein. Cell lysates were incubated in HEPES lysis buffer, pH 8.0, or lysis buffer containing either 1 M NaCl, 100 mM Na_2CO_3 or 1% Triton X-100, and fractionated at 100 000 *g* into pellets (P) and supernatants (S).

between the contractile vacuole and the plasma membrane. Contractile vacuoles are specialized organelles in protists living under hypo-osmotic conditions. Since drainin specifically serves a function at the contractile vacuole to expel water into the environment, it was unexpected that open reading frames of related proteins exist in *S.pombe*, *C.elegans* and man. This means that drainin family members are present in organisms whose osmoregulation is based on mechanisms other than the periodic discharge of water from specialized vacuoles. No function for the drainin homologs discovered in genome sequencing projects is known. *Dictyostelium* drainin thus turns out to be the first functionally characterized member of a new family of eukaryotic proteins.

The product of the human KIAA0608 gene consists of 775 amino acid residues (Wilson *et al*., 1994) and is thus 337 residues longer than the *Dictyostelium* protein (Figure 8). This human protein shares 39% of amino acid residues in its C-terminal half with *Dictyostelium* drainin; in its N-terminal domain, it exhibits no significant homology to any other known protein. The unique N-terminal domain might be a specific docking sequence or a pre-sequence cleaved off from the drainin homology portion in an activation process. Other genes encoding homologs of

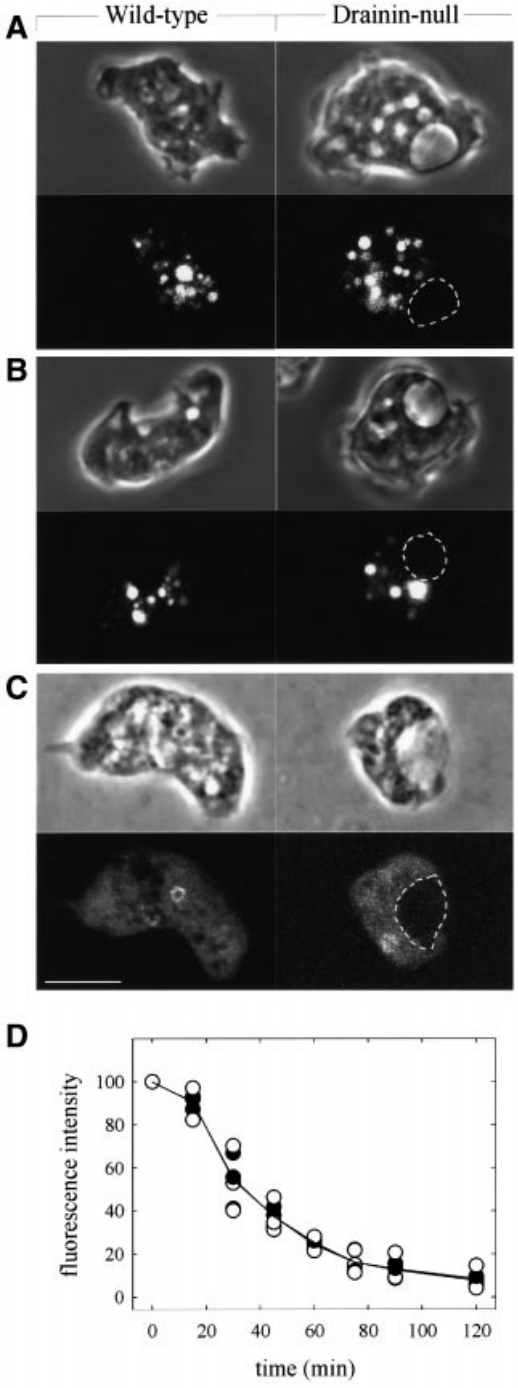

Fig. 6. Normal activities in the endocytic pathway of drainin-null cells. (**A**–**C**) Pairs of phase-contrast images (top panels) and fluorescence markers of the endocytic pathway (bottom panels) in wild-type and drainin-null cells. Living cells were pre-incubated with either TRITC–dextran (A) or neutral red (B), or fixed cells were labeled with anti-vacuolin antibody (C). None of the fluorescence markers labeled the expanded vacuole in drainin-null cells (interrupted lines). Bar = 10 μm. (**D**) Quantification of fluid-phase exocytosis from endosomes. Wild-type (●) or drainin-null (○) cells were pre-incubated with TRITC–dextran for 3 h, washed and shaken in nutrient medium. Fluorescence intensities from three independent experiments are plotted in arbitrary units (initial value = 100).

Dictyostelium drainin are yk99b4.3 of *C.elegans* (Nagase *et al*., 1998) and C23D3.03C of *S.pombe* (Niblett,D., Harris,D., Barrell,B.G., Rajandream,M.A. and Walsh,S.V. (1995) DDBJ/EMBL/GenBank accession No. Q09844). A candidate distantly related protein in *Saccharomyces cerevisiae* is the product of the YPL249c gene [Pohl,T.M. (1995) DDBJ/EMBL/GenBank accession No. S61015].

The homology between *Dictyostelium* drainin and the *C.elegans* protein extends over nearly the entire sequence, whereas the drainin homolog of *S.pombe* lacks 38 amino acids at its C-terminus. The *Dictyostelium* protein is distinguished from the other known family members by a spacer of 13 amino acids, which includes nine hydroxy-amino acids and a tandem of two proline residues.

Dictyostelium drainin is distributed as a peripheral membrane protein between cytosolic and particle fractions (Figure 5D). Accordingly, neither the *Dictyostelium* prototype nor other family members have an N-terminal hydrophobic leader sequence. A stretch of eight hydrophobic amino acids in the C-terminal half of *Dictyostelium* drainin is essential for its binding to the vacuolar membrane and for its function *in vivo*. Similar stretches of hydrophobic amino acids in the other known members of the drainin family suggest that all these proteins act by binding to the cytoplasmic phase of organelle membranes. A search for the localization of drainin homologs in higher eukaryotes might specify, as in *Dictyostelium*, a distinct vesicular compartment in *C.elegans* or mammalian cells.

Drainin distinguishes the contractile vacuole from endosomal vesicles

In its restriction to the vacuolar compartment, drainin differs from two other proteins present in the same compartment, H^+-ATPase (Heuser *et al*., 1993) and the rab4-like small GTPase rabD (Bush *et al*., 1994). These proteins are shared by the contractile vacuole system and vesicles of the endosomal pathway. Double-labeling of cells with GFP–drainin and the endosomal marker TRITC–dextran did not reveal any passage of fluid from endosomes into the vacuolar network (Figure 7B). This observation indicates that *in vivo* the two vesicle systems are tightly separated from each other, at least under the conditions used by us.

Drainin-null cells are impaired only in the discharge of contractile vacuoles, not, however, in the exocytosis of endosomes (Figure 6D). In accord with the functional distinction of the contractile vacuole and endocytic systems, vacuolin B, a protein regulating the late endocytic pathway (Jenne *et al*., 1998), is not detectable at the contractile vacuoles (Figure 6C). Vacuolins and drainin exemplify a group of proteins that shuttle between the cytoplasm and membranes of specific vesicles, thereby controlling the function of the organelles to which they bind. Comparable with the hydrophobic sequence required for the membrane binding of drainin, a stretch of hydrophobic amino acid residues is found in vacuolin B, but additional sequence motifs are supposed to be responsible for targeting these proteins either to the contractile vacuole or to vesicles of the endosomal pathway.

In the process of vacuole discharge, the vacuolar and plasma membranes are connected by a channel that persists for 3–5 s, which might allow transfer of membrane proteins from the vacuole to the cell surface. Drainin, however, is entrapped at the contractile vacuole (Figure 7A). This finding is consistent with electron microscopic data arguing against an incorporation of the vacuolar membrane into the plasma membrane (Heuser *et al*.,

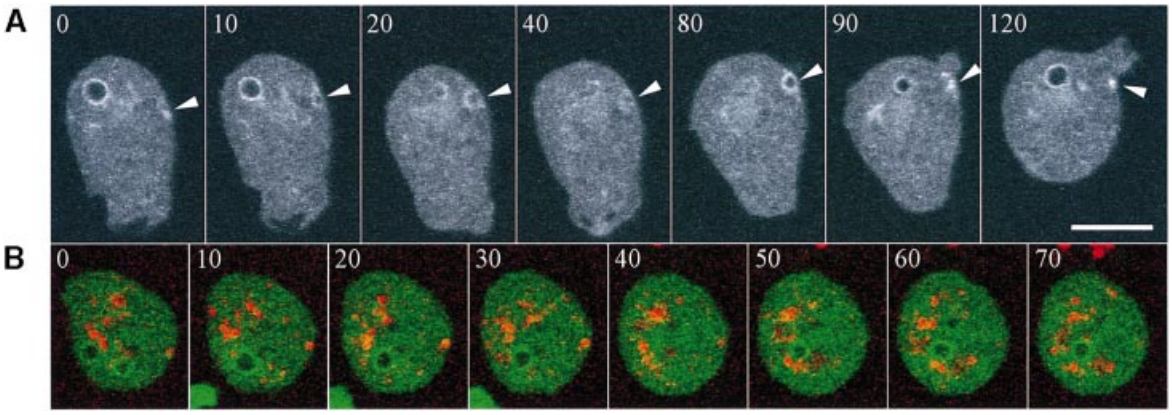

Fig. 7. Localization of GFP–drainin and endosomal marker during the contractile vacuole cycle. (**A**) GFP–drainin remains accumulated at the site of the vacuole during its entire contraction/dilatation cycle (arrowheads). (**B**) In a cell pre-loaded with TRITC–dextran for 3 h, endosomes labeled with the fluid-phase marker (red) remain separate from the contractile vacuole decorated with GFP–drainin (green) at all stages of its activity. Numbers are seconds after the beginning of the time series. Bar = 10 μm.

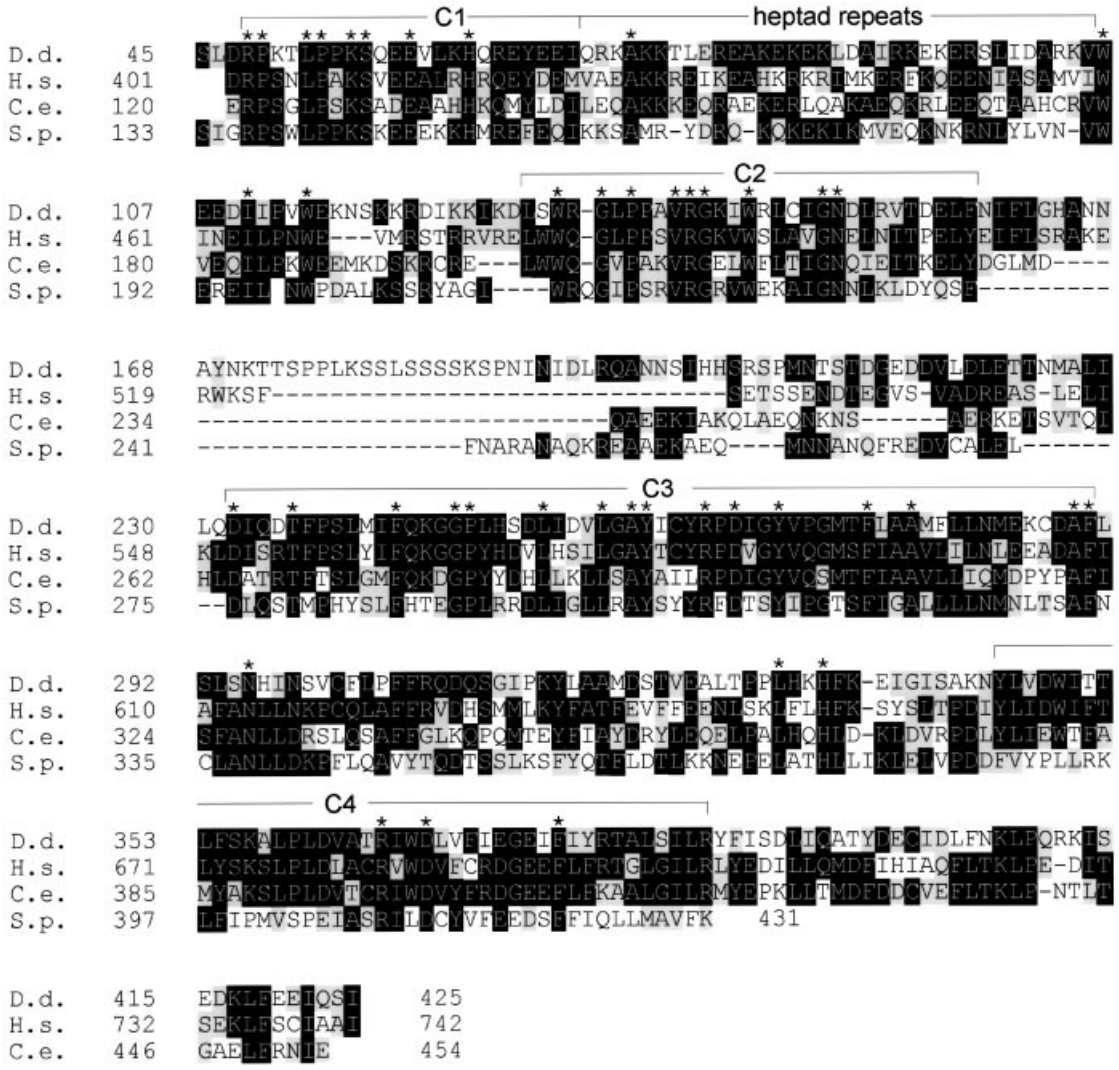

Fig. 8. Sequence comparison of drainin family members. The *Dictyostelium* drainin sequence (DDBJ/EMBL/GenBank accession No. U81500) is aligned with deduced sequences from man (KIAA0608, DDBJ/EMBL/GenBank accession No. AB011180), *C.elegans* (yk99b4.3, DDBJ/EMBL/GenBank accession No. U42831) and *S.pombe* (C23D3.03C, DDBJ/EMBL/GenBank accession No. Q09844). Identical amino acids are on a black and homologous amino acids on a gray background. Gaps (–) are introduced to optimize the sequence alignment. Stars indicate residues conserved in all family members. Clusters of sequence homology are designated C1–C4.

1993). Thus drainin does not participate in any recycling that might occur between vacuolar and plasma membranes, as has been suggested for PAT1, a Ca^{2+}-ATPase associated with both membranes (Moniakis *et al*., 1999).

Characteristics of the drainin-null phenotype

Drainin-null cells are particularly sensitive to hypo-osmotic shock (Figure 4). The generation of a regular channel between the contractile vacuole and the plasma membrane is replaced in the absence of drainin by the mechanical disruption of the lamella formed by the adjacent vacuolar and plasma membranes. This primitive method of discharge in drainin-null mutants is a normal process in *Actinosphaerium eichhorni*. In this fresh-water heliozoon, vacuoles simply enter into blebs at the cell surface and expel their contents by disruption of a thin lamella separating the vacuole from the environment (Doflein and Reichenow, 1953).

The drainin-null phenotype characterized by extremely dilated vacuoles contrasts sharply with the effects of two other mutations in the function of contractile vacuoles. In *Dictyostelium* cells overexpressing a dominant-negative form of rabD, two markers of the contractile vacuole, calmodulin and H^+-ATPase, form dense clusters near to the plasma membrane (Bush *et al*., 1996). These clusters correspond to the GFP–drainin label in the 90 and 120 s frames of the contraction cycle in Figure 7A, indicating that the contractile vacuoles are arrested in a collapsed rather than an expanded state. Similarly, in clathrin heavy chain-deficient cells, no translucent contractile vacuoles are seen (O'Halloran and Anderson, 1992).

A deficiency in discharge of the contractile vacuole may occur for one of two reasons: either no channel is formed or insufficient force is generated to press the water out. Association of myosins with the vacuole system in *Dictyostelium* (Hammer *et al*., 1996) and *Acanthamoeba* (Doberstein *et al*., 1993) suggests an actin–myosin-based mechanism for pressure generation at the vacuole. Calmodulin, which serves as a regulatory light chain in many myosins, is a marker of the contractile vacuole (Zhu and Clarke, 1992). Although none of the myosins tested so far proved to be essential for emptying of the contractile vacuole (Novak *et al*., 1995; Hammer *et al*., 1996; Jung *et al*., 1996; Temesvari *et al*., 1996), one of the other myosins in *Dictyostelium* cells might be needed for vacuole contraction.

In drainin-null cells, the vacuolar membrane is tightly aligned with the plasma membrane over a large area of its surface, so that the vacuoles are forced to assume a crescent shape (Figure 3D and E). Evacuation of these vacuoles through mechanical rupture in a hypo-osmotic environment clearly shows that the internal pressure is more than sufficient for discharge. It is therefore not a force-generating mechanism but the formation of a regular channel which is impaired in drainin-null cells.

Which step in the formation of membrane channels is blocked in drainin-null cells?

A gap of 20–50 nm width between vacuolar and plasma membrane is populated in drainin-null cells by actin filaments and bridged by proteins forming palisade-like arrays. Such arrays are common to attachment plaques where they act as spacers between pre-fusion membranes (Franke *et al*., 1976), for instance between the contractile vacuole and plasma membrane in the Trypanosomatid, *Leptomonas collosoma* (Linder and Staehelin, 1979). In veils formed at the surface of mammalian cells, these spacers are arranged into a paracrystalline hexagonal lattice (Franke *et al*., 1978).

From the presence of proteins in the inter-membrane space, it is concluded that drainin acts at an intermediate step of channel formation after attachment plaques are formed and before membrane fusion is initiated. Drainin may eliminate the actin filaments from the inter-membrane space or it may remove the palisade array of spacers. Blockage of membrane fusion by actin has been demonstrated in chromaffin cells, where two actin-depolymerizing agents, cytochalasin B and scinderin, enhance exocytosis (Furuichi *et al*., 1986; Zhang *et al*., 1996). In the drainin-null mutants of *Dictyostelium*, 10 μM cytochalasin A, which is sufficient to partially depolymerize actin filaments *in vivo*, did not restore the discharge of vacuoles (unpublished results). It seems more likely, therefore, that drainin signals to the palisade array of spacers in order to pave the way for membrane fusion.

In wild-type cells, discharge is triggered invariantly when the bladder reaches a defined size (Table I). The large volume of vacuoles in drainin-null cells implies that the connecting ducts supply sufficient membrane area to allow further expansion, which means that there is an inherent control system that limits the size of vacuoles in wild-type cells. Drainin might be involved in this control by generating a signal for channel formation and discharge of the vacuoles. This would mean that drainin acts in a volume-sensing device that triggers membrane fusion, rather than in the membrane fusion machinery itself.

It will be the goal of a detailed analysis of the *C.elegans* and human drainin homologs to define the common aspects in the function of this protein family in eukaryotes, and to specify the diversification that has accompanied metazoan evolution. The fact that the human homolog has an N-terminal extension of 400 amino acids not shared by the other known homologs deserves special attention. Since the sequence of this N-terminal domain shows no homology to other proteins in the database, efforts have to be split into the functional analysis of drainin homology domains and domains that are facultatively linked to them.

Materials and methods

Cloning of drainin

REMI mutagenesis was performed as described by Kuspa and Loomis (1992). Genomic DNA of the REMI mutant HG1648 was isolated according to Noegel *et al*. (1985), digested with *Eco*RV and religated. Subsequent transformation into *Escherichia coli* and ampicillin selection yielded a clone containing 398 bp of the drainin-coding region. This partial sequence was used to probe a λgt11 cDNA library (Clontech Inc., Palo Alto, CA). The inserts of positive clones were amplified and sequenced using drainin-specific and λgt11-specific primers. Thereby, the partial sequence of drainin was extended in the 5′ and 3′ directions. To clone the 5′ and 3′ ends of the drainin gene, genomic DNA of wild-type AX2 was digested with *Ssp*I, circularized and used as a template for inverted PCR (Ochman *et al*., 1988). The full-length coding region of drainin was compiled from overlapping sequences of cDNA clones and PCR-generated genomic fragments in plus and minus end directions. Custom sequencing was performed by Toplab (Martinsried, Germany) on a Perkin Elmer Cycle Sequencer (ABI377). Database analysis was carried out using the Gapped BLAST program (Altschul *et al*., 1997).

Generation of drainin-null mutants

The targeting vector was constructed by replacing bp 416–424 of the drainin-coding region with the blasticidin-S resistance (Bsr) cassette of pBsr2 (Sutoh, 1993). A PCR-based genomic fragment encompassing bp 425–1547 of drainin was amplified using primers 5′-gcgtctagacacaagaggaagtattaaaacatc and 5′-gcgaattcctttggtctaaaactattgactg, and linked by an *Xba*I site to the Bsr cassette of pBsr2. A second PCR fragment of drainin comprising bp –153 to 415 was generated using primers 5′-cgcggatccagccatatcaaaaagtagtggag and 5′-cgcaagcttgtaatgtttttggtctatccaatg, and cloned in pGEM7zf+ (Promega) at *Bam*HI and *Hin*dIII sites. The final targeting vector was assembled by subcloning the *Eco*RI–*Hin*dIII fragment, which contained the first PCR fragment and the Bsr cassette, into the pGEM7zf+.

The gene replacement construct was excised using *Eco*RI and *Bam*HI, and the linearized and dephosphorylated fragment was used to transform by electroporation (Howard *et al*., 1988) the *Dictyostelium* AX2 wild-type strain and mutant HG592 (Gerisch *et al*., 1985), the parental strain of HG1648. Drainin-null cells were selected with 5 μg/ml blasticidin-S (ICN Biomedicals, Inc., Costa Mesa, CA) in nutrient medium.

For Southern blot analysis, 10 μg of either AX2 or mutant DNA was digested with *Cla*I, separated on a 1% agarose gel and transferred onto Hybond N nylon membrane (Amersham, Little Chalfont, UK). The blots were hybridized under high stringency for 4 h at 65°C in RapidHyb buffer (Amersham) with a PCR-generated probe comprising bp 425–1547 of the drainin-coding region.

For Northern blot analysis, total RNA of AX2, HG1648 and two independent drainin-null mutants was isolated following the procedure of Mehdy *et al*. (1983) and run on a 1% agarose gel. A PCR-based fragment encompassing bp –154 to 577 of drainin was used for hybridization.

Strains and culture conditions

Cells of *Dictyostelium* wild-type AX2-214, HG592 (Gerisch *et al*., 1985) and transformants derived from these strains were cultivated axenically in nutrient medium. The cells were harvested from suspension cultures shaken at 150 r.p.m. during exponential growth at a cell density of $<5\times10^6$/ml (Claviez *et al*., 1982). Clones producing GFP fusions were cultivated in the same medium supplemented with 20 μg/ml of geneticin (G418). Prior to fluorescence imaging, the cells were placed on a coverslip and washed five times in 17 mM K/Na phosphate buffer, pH 6.0. All experiments with living cells were performed at 23°C.

Electron microscopy

For Epon embedding, cells were fixed for 15 min in suspension at room temperature followed by 45 min on ice in 17 mM K/Na phosphate buffer, pH 6.0, containing 2% glutaraldehyde and 0.2% osmium tetroxide (Franke *et al*., 1969). After staining for 1 h on ice with 1% uranyl acetate according to Griffiths (1993), the cells were dehydrated with ethanol and embedded in Epon. Sections of 70 nm were stained with 3% lead citrate and 4% uranyl acetate, and micrographs taken on a JEM 100 CX transmission electron microscope (Jeol) on Scienta EM film (Agfa).

For cryo-electron microscopy, cells were fixed for 15 min at room temperature in a solution containing 15% (v/v) saturated picric acid, 2% paraformaldehyde, 0.2% acrolein and 10 mM PIPES–HCl, pH 6.0. Fixed cells were embedded in gelatine blocks infused with 1.8 M sucrose in polyvinylpyrrolidone. Specimens were cryosectioned essentially as described by Tokuyasu (1989), and 70 nm sections were pre-incubated with 2% fish gelatine, incubated overnight with 5 μg/ml of anti-actin mAb 224-236-1 (Hanakam *et al*., 1996) and labeled with 9 μg/ml of rabbit anti-mouse-IgG antibodies (Jackson ImmunoResearch, code 315-005-048) followed by protein A conjugated to 10 nm gold (BioCell, Cardiff, UK), post-fixed with 2% glutaraldehyde, stained and photographed as for Epon sections.

Osmotic shock treatment

AX2 wild-type and mutant cells were incubated for 1 h in 17 mM K/Na phosphate buffer, pH 6.0, at a density of 1×10^7 cells/ml, followed by 2 h of incubation in either the phosphate buffer, distilled water or 0.4 M sorbitol in phosphate buffer (Rivero *et al*., 1996; Schuster *et al*., 1996). For a control, cells were exposed to 130 mM sucrose. After adjustement to 2×10^2 cells/ml in phosphate buffer containing 10 mM EDTA to prevent cell aggregation, 100 μl of cell suspension were plated immediately on SM agar with *Klebsiella aerogenes*. The survival rate was estimated by counting colonies after 3 days of growth at 23°C. To analyze cell morphology after osmotic shock treatment, cells were placed on glass coverslips and recorded under agar overlay (Yumura *et al*., 1984) by phase-contrast microscopy.

Quantification of exocytosis

The rate of exocytosis from the endocytic compartment was measured essentially as described (Klein and Satre, 1986; Maniak *et al*., 1995; Hacker *et al*., 1997). A total of 1×10^7 cells were incubated in 10 ml of nutrient medium containing TRITC–dextran (4 mg/ml) in 25 ml Erlenmeyer flasks at 150 r.p.m. After 3 h, cells were washed once and resuspended in 10 ml of nutrient medium. Samples of 1 ml were withdrawn at intervals, added to 100 μl of trypan blue to quench extracellular fluorescence, and centrifuged for 3 min at 500 *g*. Pellets were resuspended in 1 ml of 17 mM K/Na phosphate buffer, pH 6.0, and TRITC fluorescence was measured immediately in a Kontron SFM 25 fluorescence spectrometer at 544 nm for excitation and 574 nm for emission.

Immunofluorescence microscopy

Cells were allowed to adhere to glass coverslips for 30 min. The cells were fixed with picric acid and paraformaldehyde and post-fixed with 70% ethanol according to Humbel and Biegelmann (1992), labeled with monoclonal antibody 2D1 against calmodulin (Zhu and Clarke, 1992), mAb 221-35-2 against the H^+-ATPase (Jenne *et al*., 1998) or mAb 221-1-1 against vacuolin (Rauchenberger *et al*., 1997), followed by TRITC-conjugated goat anti-mouse IgG (Dianova, Hamburg, Germany). Specimens were scanned on a Zeiss LSM 410 laser scanning confocal microscope equipped with a 543 nm HeNe Laser and a Zeiss 100/1.3 Plan-Neofluar objective. Data were processed and images false-colored using AVS software (Advanced Visual Systems, Waltham, MA).

Fluorescence recording in living cells of GFP, GFP–drainin fusions and endosomal markers

The GFP- and GFP–drainin-producing strains were obtained by transformation of drainin-null cells with pDNeogfp-based vectors (Rauchenberger *et al*., 1997) and by selection in nutrient medium with 20 μg/ml G418. Inserts contained either the coding region of *Aequorea victoria* GFP (Prasher *et al*., 1992) or an in-frame fusion of GFP and the full-length drainin-coding region. For a GFP–drainin fusion protein missing the hydrophobic domain of amino acid residues 275–282, a 5′ fragment comprising bp 1–822 was ligated at a *Kpn*I site to a 3′-terminal fragment comprising bp 849–1314, and cloned into pDNeogfp. In these constructs, transcription of the inserts was driven by the actin-6 promoter of *Dictyostelium*.

Time series of GFP fluorescence distributions were obtained by scanning confocal sections at intervals of 8 s using a Zeiss LSM 410 confocal microscope and the agar overlay technique (Yumura *et al*., 1984). For Figures 6A and 7B, cells were incubated for 3 h in nutrient medium containing TRITC–dextran at a concentration of 4 mg/ml, placed on a coverslip and washed five times with 17 mM K/Na phosphate buffer, pH 6.0. For Figure 6B, cells were exposed in the same buffer to 0.5 mM neutral red for 5 min.

Protein extraction and Western blotting

Cells washed in 17 mM K/Na phosphate buffer, pH 6.0, were resuspended and lysed in 50 mM HEPES buffer, pH 8.0, containing 50 mM NaCl, 1 mM EDTA, 1 mM EGTA and protease inhibitors (Westphal *et al*., 1997). Total cell lysates were incubated in the lysis buffer supplemented either with 1 M NaCl, 1% Triton X-100 or 100 mM Na_2CO_3. Extracts were fractionated at 100 000 *g* into pellet and supernatant, and analyzed by SDS–PAGE. Western blots were probed overnight with anti-GFP mAb 264-449-3 (Jenne *et al*., 1998) or anti-calnexin mAb 270-349-1 (courtesy of Mary Ecke, Martinsried), and subsequently with goat anti-mouse IgG antibodies conjugated to alkaline phosphatase (Jackson ImmunoResearch, West Grove, PA).

Accession number

The drainin genomic DNA sequence has been deposited in the DDBJ/EMBL/GenBank database under the accession No. U81500.

Acknowledgements

We thank Margaret Clarke, Mary Ecke and Markus Maniak for antibodies, and Markus Maniak for the introduction to phagocytosis assays.

References

Allen,C.A. and Green,D.P.L. (1997) The mammalian acrosome reaction: gateway to sperm fusion with the oocyte? *BioEssays*, **19**, 241–247.

Altschul,S.F., Madden,T.L., Schäffer,A.A., Zhang,J., Zhang,Z., Miller,W. and Lipman,D.J. (1997) Gapped BLAST and PSI-BLAST: a new generation of protein database search programs. *Nucleic Acids Res.*, **25**, 3389–3402.

Bennett,M.K. (1995) SNAREs and the specificity of transport vesicle targeting. *Curr. Opin. Cell Biol.*, **7**, 581–586.

Bush,J., Nolta,K., Rodriguez-Paris,J., Kaufmann,N., O'Halloran,T., Ruscetti,T., Temesvari,L., Steck,T. and Cardelli,J. (1994) A Rab4-like GTPase in *Dictyostelium discoideum* colocalizes with V-H^+-ATPases in reticular membranes of the contractile vacuole complex and in lysosomes. *J. Cell Sci.*, **107**, 2801–2812.

Bush,J., Temesvari,L., Rodriguez-Paris,J., Buczynski,G. and Cardelli,J. (1996) A role for a Rab4-like GTPase in endocytosis and in regulation of contractile vacuole structure and function in *Dictyostelium discoideum*. *Mol. Biol. Cell*, **7**, 1623–1638.

Caohuy,H., Srivastava,M. and Pollard,H.B. (1996) Membrane fusion protein synexin (annexin VII) as a Ca^{2+}/GTP sensor in exocytotic secretion. *Proc. Natl Acad. Sci. USA*, **93**, 10797–10802.

Cardelli,J.A., Richardson,J. and Miears,D. (1989) Role of acidic intracellular compartments in the biosynthesis of *Dictyostelium* lysosomal enzymes. The weak bases ammonium chloride and chloroquine differentially affect proteolytic processing and sorting. *J. Biol. Chem.*, **264**, 3454–3463.

Clarke,M. and Heuser,J. (1997) Water and ion transport. In Maeda,Y., Inouye,K. and Takeuchi,I. (eds), *Dictyostelium. A Model System for Cell and Developmental Biology.* Frontiers Science No. 21. Universal Academy Press, Inc., Tokyo, Japan, pp. 75–91.

Claviez,M., Pagh,K., Maruta,H., Baltes,W., Fisher,P. and Gerisch,G. (1982) Electron microscopic mapping of monoclonal antibodies on the tail region of *Dictyostelium* myosin. *EMBO J.*, **1**, 1017–1022.

Doberstein,S.K., Baines,I.C., Wiegand,G., Korn,E.D. and Pollard,T.D. (1993) Inhibition of contractile vacuole function *in vivo* by antibodies against myosin I. *Nature*, **365**, 841–843.

Doflein,F., and Reichenow,E. (1953) Allgemeine Morphologie und Physiologie der Protozoen. In Doflein,F. and Reichenow,E. (eds), *Lehrburch der Protozoenkunde*. VEB Gustav Fischer Verlag, Jena, Germany, p. 13.

Emans,N., Gorvel,J.P., Walter,C., Gerke,V., Kellner,R., Griffiths,G. and Gruenberg,J. (1993) Annexin II is a major component of fusogenic endosomal vesicles. *J. Cell Biol.*, **120**, 1357–1369.

Franke,W.W., Krien,S. and Brown,R.M.,Jr (1969) Simultaneous glutaraldehyde–osmium tetroxide fixation with postosmication. *Histochemie*, **19**, 162–164.

Franke,W.W., Luder,M.R., Kartenbeck,J., Zerban,H. and Keenan,T.W. (1976) Involvement of vesicle coat material in casein secretion and surface regeneration. *J. Cell Biol.*, **69**, 173–195.

Franke,W.W., Grund,C., Schmid,E. and Mandelkow,E. (1978) Paracrystalline arrays of membrane-to-membrane cross bridges associated with the inner surface of plasma membrane. *J. Cell Biol.*, **77**, 323–328.

Furuichi,K., Ra,C., Isersky,C. and Rivera,J. (1986) Comparative evaluation of the effect of pharmacological agents on endocytosis and coendocytosis of IgE by rat basophilic leukaemia cells. *Immunology*, **58**, 105–110.

Geppert,M. and Südhof,T.C. (1998) RAB3 and synaptotagmin: the yin and yang of synaptic membrane fusion. *Annu. Rev. Neurosci.*, **21**, 75–95.

Gerisch,G., Hagmann,J., Hirth,P., Rossier,C., Weinhart,U. and Westphal,M. (1985) Early *Dictyostelium* development: control mechanisms bypassed by sequential mutagenesis. *Cold Spring Harbor Symp. Quant. Biol.*, **50**, 813–822.

Giglione,C. and Gross,J.D. (1995) Anion effects on vesicle acidification in *Dictyostelium*. *Biochem. Mol. Biol. Int.*, **36**, 1057–1065.

Gingell,D., Todd,I. and Owens,N. (1982) Interaction between intracellular vacuoles and the cell surface analysed by finite aperture theory interference reflection microscopy. *J. Cell Sci.*, **54**, 287–298.

Griffiths,G. (ed.) (1993) *Fine Structure Immunocytochemistry.* Springer Verlag, Berlin, Germany.

Hacker,U., Albrecht,R. and Maniak,M. (1997) Fluid-phase uptake by macropinocytosis in *Dictyostelium*. *J. Cell Sci.*, **110**, 105–112.

Hammer,J., Lydan,M. and Jung,G. (1996) *Dictyostelium* MyoJ associates with membranes of the contractile vacuole complex. *Mol. Biol. Cell*, **7**, 374a, abstract 2174.

Hanakam,F., Albrecht,R., Eckerskorn,C., Matzner,M. and Gerisch,G. (1996) Myristoylated and non-myristoylated forms of the pH sensor protein hisactophilin II: intracellular shuttling to plasma membrane and nucleus monitored in real time by a fusion with green fluorescent protein. *EMBO J.*, **15**, 2935–2943.

Hanson,P.I., Heuser,J.E. and Jahn,R. (1997) Neurotransmitter release—four years of SNARE complexes. *Curr. Opin. Neurobiol.*, **7**, 310–315.

Heuser,J., Zhu,Q. and Clarke,M. (1993) Proton pumps populate the contractile vacuoles of *Dictyostelium* amoebae. *J. Cell Biol.*, **121**, 1311–1327.

Howard,P.K., Ahern,K.G. and Firtel,R.A. (1988) Establishment of a transient expression system for *Dictyostelium discoideum*. *Nucleic Acids Res.*, **16**, 2613–2623.

Hughson,F.M. (1997) Enveloped viruses: a common mode of membrane fusion? *Curr. Biol.*, **7**, R565–R569.

Humbel,B.M. and Biegelmann,E. (1992) A preparation protocol for postembedding immunoelectron microscopy of *Dictyostelium discoideum* cells with monoclonal antibodies. *Scanning Microsc.*, **6**, 817–825.

Jenne,N., Rauchenberger,R., Hacker,U., Kast,T. and Maniak,M. (1998) Targeted gene disruption reveals a role for vacuolin B in the late endocytic pathway and exocytosis. *J. Cell Sci.*, **111**, 61–70.

Jung,G., Wu,X. and Hammer,J.A.,III (1996) *Dictyostelium* mutants lacking multiple classic myosin I isoforms reveal combinations of shared and distinct functions. *J. Cell Biol.*, **133**, 305–323.

Klein,G. and Satre,M. (1986) Kinetics of fluid-phase pinocytosis in *Dictyostelium discoideum* amoebae. *Biochem. Biophys. Res. Commun.*, **138**, 1146–1152.

Kuspa,A. and Loomis,W.F. (1992) Tagging developmental genes in *Dictyostelium discoideum* by restriction enzyme-mediated integration of plasmid DNA. *Proc. Natl Acad. Sci. USA*, **89**, 8803–8807.

Linder,J.C. and Staehelin,L.A. (1979) A novel model for fluid secretion by the trypanosomatid contractile vacuole apparatus. *J. Cell Biol.*, **83**, 371–382.

Liu,T. and Clarke,M. (1996) The vacuolar proton pump of *Dictyostelium discoideum*: molecular cloning and analysis of the 100 kDa subunit. *J. Cell Sci.*, **109**, 1041–1051.

Maniak,M., Rauchenberger,R., Albrecht,R., Murphy,J. and Gerisch,G. (1995) Coronin involved in phagocytosis: dynamics of particle-induced relocalization visualized by a green fluorescent protein tag. *Cell*, **83**, 915–924.

Mehdy,M.C., Ratner,D. and Firtel,R.A. (1983) Induction and modulation of cell-type-specific gene expression in *Dictyostelium*. *Cell*, **32**, 763–771.

Moniakis,J., Coukell,B. and Janiec,A. (1999) Involvement of the Ca^{2+} ATPase PAT1 and the contractile vacuole in calcium regulation in *Dictyostelium discoideum*. *J. Cell Sci.*, **112**, 405–414.

Muallem,S., Kwiatkowska,K., Xu,X. and Yin,H.L. (1995) Actin filament disassembly is a sufficient final trigger for exocytosis in nonexcitable cells. *J. Cell Biol.*, **128**, 589–598.

Nagase,T., Ishikawa,K., Miyajima,N., Tanaka,A., Kotani,H., Nomura,N. and Ohara,O. (1998) Prediction of the coding sequences of unidentified human genes. IX. The complete sequences of 100 new cDNA clones from brain which can code for large proteins *in vitro*. *DNA Res.*, **5**, 31–39.

Noegel,A., Welker,D.L., Metz,B.A. and Williams,K.L. (1985) Presence of nuclear associated plasmids in the lower eukaryote *Dictyostelium discoideum*. *J. Mol. Biol.*, **185**, 447–450.

Nolta,K.V. and Steck,T.L. (1994) Isolation and initial characterization of the bipartite contractile vacuole complex from *Dictyostelium discoideum*. *J. Biol. Chem.*, **269**, 2225–2233.

Nolta,K.V., Rodriguez-Paris,J.M. and Steck,T.L. (1994) Analysis of successive endocytic compartments isolated from *Dictyostelium discoideum* by magnetic fractionation. *Biochim. Biophys. Acta*, **1224**, 237–246.

Novak,K.D., Peterson,M.D., Reedy,M.C. and Titus,M.A. (1995) *Dictyostelium* myosin I double mutants exhibit conditional defects in pinocytosis. *J. Cell Biol.*, **131**, 1205–1221.

Ochman,H., Gerber,A.S. and Hartl,D.L. (1988) Genetic application of an inverse polymerase chain reaction. *Genetics*, **120**, 621–623.

O'Halloran,T.J. and Anderson,R.G.W. (1992) Clathrin heavy chain is required for pinocytosis, the presence of large vacuoles, and development in *Dictyostelium*. *J. Cell Biol.*, **118**, 1371–1377.

Prasher,D.C., Eckenrode,V.K., Ward,W.W., Prendergast,F.G. and Cormier,M.J. (1992) Primary structure of the *Aequorea victoria* green fluorescent protein. *Gene*, **111**, 229–233.

Rauchenberger,R., Hacker,U., Murphy,J., Niewöhner,J. and Maniak,M. (1997) Coronin and vacuolin identify consecutive stages of a late, actin-coated endocytic compartment in *Dictyostelium*. *Curr. Biol.*, **7**, 215–218.

Rivero,F., Köppel,B., Peracino,B., Bozzaro,S., Siegert,F., Weijer,C.J., Schleicher,M., Albrecht,R. and Noegel,A.A. (1996) The role of the cortical cytoskeleton: F-actin crosslinking proteins protect against osmotic stress, ensure cell size, cell shape and motility, and contribute to phagocytosis and development. *J. Cell Sci.*, **109**, 2679–2691.

Rothman,J.E. (1994) Intracellular membrane fusion. *Adv. Second Messenger Phosphoprotein Res.*, **29**, 81–96.

Rybin,V., Ullrich,O., Rubino,M., Alexandrov,K., Simon,I., Seabra,M.C., Goody,R. and Zerial,M. (1996) GTPase activity of Rab5 acts as a timer for endocytic membrane fusion. *Nature*, **383**, 266–269.

Sato,K. and Wickner,W. (1998) Functional reconstitution of ypt7p GTPase and a purified vacuole SNARE complex. *Science*, **281**, 700–702.

Schiavo,G., Gmachl,M.J.S., Stenbeck,G., Söllner,T.H. and Rothman,J.E. (1995) A possible docking and fusion particle for synaptic transmission. *Nature*, **378**, 733–736.

Schuster,S.C., Noegel,A.A., Oehme,F., Gerisch,G. and Simon,M.I. (1996) The hybrid histidine kinase DokA is part of the osmotic response system of *Dictyostelium*. *EMBO J.*, **15**, 3880–3889.

Skehel,J.J. and Wiley,D.C. (1998) Coiled coils in both intracellular vesicle and viral membrane fusion. *Cell*, **95**, 871–874.

Sutoh,K. (1993) A transformation vector for *Dictyostelium discoideum* with a new selectable marker *bsr*. *Plasmid*, **30**, 150–154.

Temesvari,L.A., Bush,J.M., Peterson,M.D., Novak,K.D., Titus,M.A. and Cardelli,J.A. (1996) Examination of the endosomal and lysosomal pathways in *Dictyostelium discoideum* myosin I mutants. *J. Cell Sci.*, **109**, 663–673.

Tokuyasu,K.T. (1989) Use of poly(vinylpyrrolidone) and poly(vinyl-alcohol) for cryoultramicrotomy. *Histochem. J.*, **21**, 163–171.

Umbach,J.A., Mastrogiacomo,A. and Gundersen,C.B. (1995) Cystein string proteins and presynaptic function. *J. Physiol.*, **89**, 95–101.

Weber,T., Zemelman,B.V., McNew,J.A., Westermann,B., Gmachl,M., Parlati,F., Söllner,T.H. and Rothman,J.E. (1998) SNAREpins: minimal machinery for membrane fusion. *Cell*, **92**, 759–772.

Westphal,M., Jungbluth,A., Heidecker,M., Mühlbauer,B., Heizer,C., Schwartz,J.-M., Marriott,G. and Gerisch,G. (1997) Microfilament dynamics during cell movement and chemotaxis monitored using a GFP–actin fusion protein. *Curr. Biol.*, **7**, 176–183.

Wilson,R. *et al*. (1994) 2.2 Mb of contiguous nucleotide sequence from chromosome III of *C.elegans*. *Nature*, **368**, 32–38.

Xu,Z., Sato,K. and Wickner,W. (1998) LMA1 binds to vacuoles at Sec18p (NSF), transfers upon ATP hydrolysis to a t-SNARE (Vam3p) complex, and is released during fusion. *Cell*, **93**, 1125–1134.

Yumura,S., Mori,H. and Fukui,Y. (1984) Localization of actin and myosin for the study of ameboid movement in *Dictyostelium* using improved immunofluorescence. *J. Cell Biol.*, **99**, 894–899.

Zhang,L., Marcu,M.G., Nau-Staudt,K. and Trifaro,J.-M. (1996) Recombinant scinderin enhances exocytosis, an effect blocked by two scinderin-derived actin-binding peptides and PIP2. *Neuron*, **17**, 287–296.

Zhu,Q. and Clarke,M. (1992) Association of calmodulin and an unconventional myosin with the contractile vacuole complex of *Dictyostelium discoideum*. *J. Cell Biol.*, **118**, 347–358.

Received March 15, 1999; revised April 20, 1999;
accepted April 21, 1999